Materials Science Forum Vols. 638-642 (2010) pp 2046-2051
Online available since 2010/Jan/12 at www.scientific.net

doi:10.4028/www.scientific.net/MSF.638-642.2046

Effect of Carbon Addition of Shape Memory Properties of TiNb Alloys

Hideki Hosoda[1,a], Y. Horiuchi[1*,b], T. Inamura[1,c], K. Wakashima[1,e]
H. Y. Kim[2,f] and S. Miyazaki[2,g]

[1]Precision and Intelligence Laboratory, Tokyo Institute of Technology,
4259-R2-27, Midori-ku, Yokohama 226-8503, Japan
[2]Institute of Materials Science, University of Tsukuba,
Tennodai 1-1-1, Tsukuba, Ibaraki 305-8573, Japan
*Graduate student, Tokyo Institute of Technology (Now with Toshiba Co. Ltd.)
[a]hosoda.h.aa@m.titech.ac.jp, [b]yosuke.horiuchi@toshiba.co.jp, [c]inamura.t.aa@m.titech.ac.jp,
[d]wakashima.k.aa@m.titech.ac.jp, [e]kim@ims.tsukuba.ac.jp, [f]miyazaki@ims.tsukuba.ac.jp

Keywords: carbon addition, shape memory properties, TiNb, strengthening, TiC, grain size, superelasticity, texture, critical stress for slip

Abstract. In order to increase critical stress for slip in Ti-Nb base shape memory alloys, strengthening by carbon additions (0.2 and 0.5mass%C) to Ti-27mol%Nb was investigated. It was found that all the alloys were β (bcc) phase at room temperature, and TiC existed in C-added alloys. The grain size was decreased with carbon content due to grain boundary pinning. Texture measurement revealed that strong $\{112\}_\beta<110>_\beta$ recrystallization texture was formed in C-free alloy and that weak $\{001\}_\beta<110>_\beta$ texture in C-added alloys. Tensile tests revealed that clear superelasticity appeared in C-free alloy but that stress-induced martensitic transformation seems to be suppressed by TiC in C-added alloys. The critical stress for slip was linearly increased by carbon content. Then, carbon addition affects the shape memory properties of TiNb alloys, and is effective to enhance the critical stress for slip.

Introduction

In order to avoid the possibility of Ni allergy and hypersensitivity, Ni-free nontoxic biomedical shape memory alloys (SMAs) are required for the medical applications [1]. Ti-based biomedical SMAs, in which shape memory effect comes from the martensitic transformation between β (bcc) and α" (c-centered orthorhombic [2, 3]), are promising and several researches have been already made from 1971 [1, 4]. Common features of the Ti-based SMAs are excellent cold workability and low values of $d\sigma_{SMST}/dT$ (4.4MPa/K for Ti-26mol%Nb [5]) in Clausius-Clapeyron equation where σ_{SMST} and T are the stress for inducing martensite and temperature, respectively. The low value of $d\sigma_{SMST}/dT$ leads to the wide temperature range of superelasticity. Now about 4% superelastic strain was reported for Ti-24mol%Nb-3mol%Al [6] and 6.5% for the Ti-18mol%Nb-6mol%Zr [7]. However, a technical breakthrough is still required for practical applications; that is hardening method for the Ti SMAs. Figure 1 show a schematic diagram of a SMA. If the critical stress for slip deformation σ_{SLIP} is lower than the stress for inducing martensitic transformation σ_{SIMT}, only permanent plastic deformation occurs instead of superelasticity. However, if the σ_{SLIP} can be raised over σ_{SIMT}, superelasticity appears. As for the TiNi SMAs, proper thermo-mechanical treatments are already established: work hardening by cold work and/or precipitation hardening by Ti_3Ni_4 [8]. Although similar hardening methods were tried for Ti-SMAs, the suitable treatment has not been found at present. Therefore, in order to increase critical stress for slip, strengthening by addition of interstitial carbon was investigated in this work.

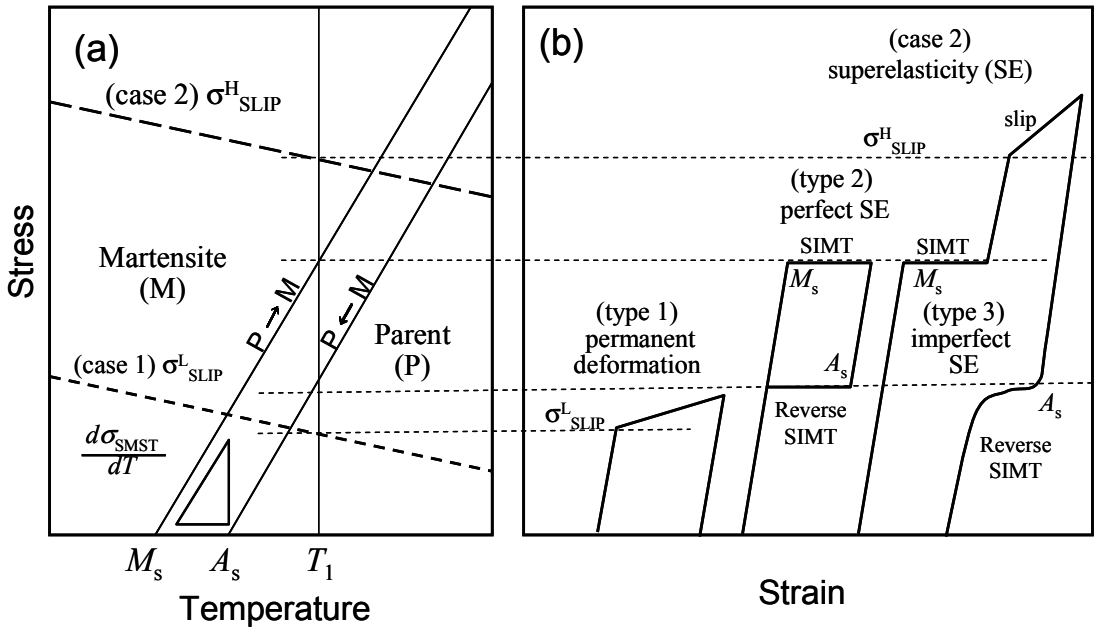

Figure 1 A schematic diagram showing phase transformation of SMA (a) and corresponding stress-strain (SS) curves (b). Two cases are shown: (case1) the critical stress for slip is low (=σ^{L}_{SLIP}) and (case2) high (=σ^{H}_{SLIP}). The test temperature is T_1. In case1, slip deformation only occurs, then, "type1" SS curve is obtained which is seen in usual metals and alloys. In case2, stress-induced martensitic transformation (SIMT) occurs prior to slip deformation. Then, superelasticity (SE) appears, and "type2" SS curve is obtained. Even in case2, when the applied stress exceeds σ^{H}_{SLIP}, slip deformation also introduced, and "type3" SS curve is obtained.

Other interstitial additions to Ti-Nb base alloys have been reported such as O [9] and B [10]. The base alloy selected was Ti-27mol%Nb in which superelasticity appears [1, 11], and 0.2 and 0.5mass%C were added. The carbon contents were comparable to the maximum carbon solubility in Ti (~0.5mass% at 1921K) and in Nb (~1mass% at 2612K) in the literature [12].

Experimental procedure

Ti-27mol%Nb (termed Ti-27Nb) was selected as a basic composition, 0.2mass%C (termed 0.2C) and 0.5mass%C (termed 0.5C) were added. The starting materials were high purity elements: 99.99% for Ti and 99.9% Nb and carbon. The ingots were fabricated by Ar arc-melting method in Ar-1%H_2 using W electrode. After alloying, no chemical analysis was made because of small weight change detected. The ingots were homogenized at 1273K for 86.4ks in vacuum followed by quenching into water. Then, the ingots were cold-rolled with final thickness of 0.1mm. The cold-rolled materials were solution-treated at 1273K for 1.8ks in vacuum followed by quenching into water.

θ-2θ X ray diffraction analysis at room temperature (RT) was done using Philips X'pert Pro Galaxy system. The measurement range was 10 to 140 degrees in 2θ with CuKα. Si external standard was used for accurate correction in peak angles. Scanning electron microscopy (SEM, Hitachi S-4300SE) combined with electron backscattering diffraction (EBSD, Oxford INCA Crystal EBSP detector) and transmission electron microscopy (TEM, Philips CM200 with an acceleration voltage of 200V) were used for microstructural characterization. For mechanical properties, cyclic loading-unloading tensile tests were carried out at RT using an Instron-type Shimazdu Autograph AG1kN. The strain increment

per cycle was 1% and the strain rate was 5.0×10^{-4}/s. The gauge length, width and thickness of the tensile specimens were 10mm, 2mm and 0.1mm, respectively. The tensile direction was parallel to the rolling direction (RD).

3. Results and Discussion

Phase constitution and microstructure.

Figure 2 shows XRD profiles of Ti-27Nb, 0.2C and 0.5C in a range from 30 to 80 degrees. The constituent phase was β (bcc) regardless of C content, and TiC was detected in both C-added alloys. The peak intensity from TiC was larger in 0.5C than in 0.2C. Therefore, the amount of TiC seems to increase with C content. Then, the solid solubility of carbon in Ti-27Nb at 1273K is judged to be less than 0.2mass%C, which was slightly lower than expected in the binary phase diagrams [12].

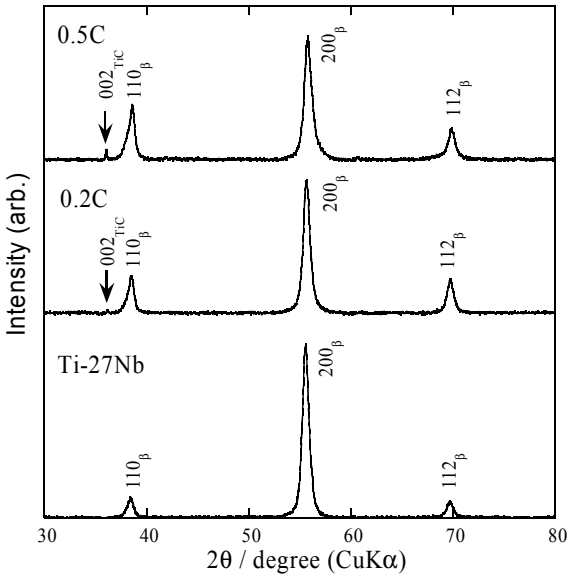

Figure 2 Partial XRD profiles of Ti-27Nb, 0.2C and 0.5C.

Figure 3 shows microstructures taken by SEM-EBSP. Equiaxied grains were formed regardless of carbon content. Then, recrystallization was completely finished by the solution treatment at 1273K for 1.8ks. The microstructures seemed single phase in Ti-27Nb, and fine grains were formed in C-added alloys. The grain size became smaller with increasing C content: 63μm for Ti-27Nb, 23μm for 0.2C and 15μm for 0.5C, respectively. Therefore, carbon addition is effective to the grain refinement in Ti-Nb alloys. Texture measurement by EBSD revealed that Ti-27Nb exhibited a strong $\{112\}_\beta<110>_\beta$ recrystallization, 0.5C exhibited a weak $\{001\}_\beta<110>_\beta$ deformation texture, and that 0.2C exhibited mixture of both textures. The texture development in the Ti-Nb-C alloys is similar to that in the Ti-Nb-Ge alloys in which $(Ti, Nb)_5Ge_3$ particles interrupt the grain boundary motion [13]. Figure 4 shows TEM bright field images of (a) Ti-27Nb and (b) 0.5C. Ti-27Nb consisted in β phase in addition to small amount of athermal ω phase with a hexagonal crystal structure [14]. On the other hand, in the C-added alloys, TiC particles existed inside of grains and at grain boundaries. The phase constitution by TEM was in good agreement with the XRD results. The lattice parameters

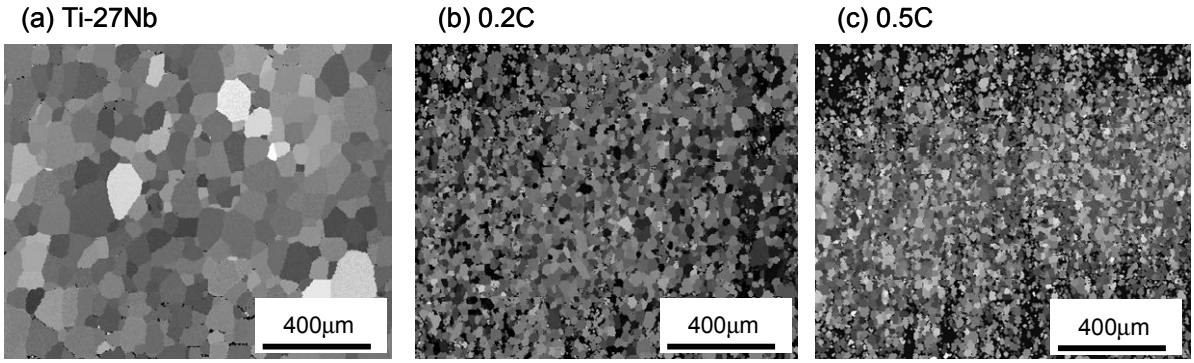

Figure 3 Microstructures obtained by SEM-EBSD: (a) Ti-27Nb, (b) 0.2C and (c) 0.5C.

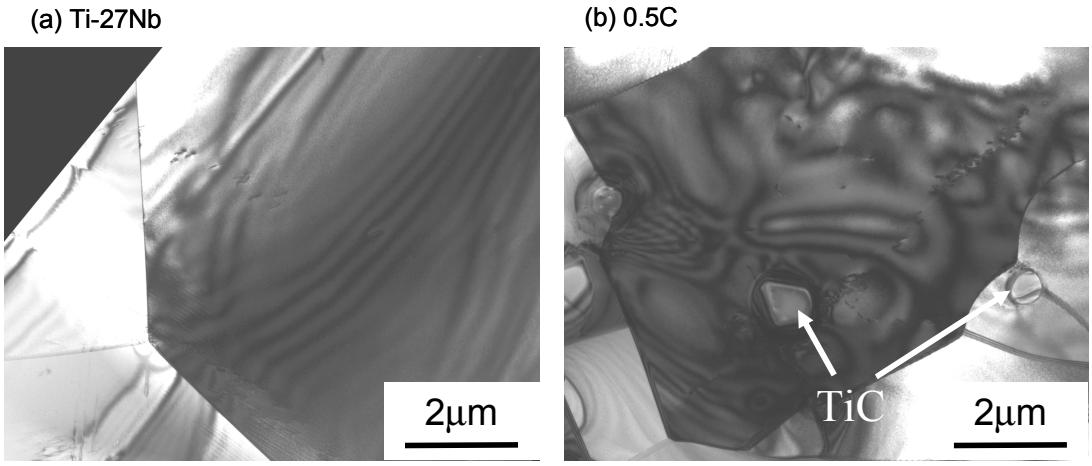

Figure 4 TEM micrographs of (a) Ti-27Nb and (b) 0.5C.

Table 1 Phase constitution, grain size and texture of Ti-27Nb, 0.2C and 0.5C.

Alloy	Phase	Average grain size	Texture
Ti-27Nb	β and ω	63μm	strong $\{112\}_\beta<110>_\beta$
0.2C	β, ω and TiC	23μm	mixture*
0.5C	β, ω and TiC	15mm	weak $\{001\}_\beta<110>_\beta$

* mixture of $\{112\}_\beta<110>_\beta$ and $\{001\}_\beta<110>_\beta$

evaluated using the XRD and TEM were 0.3283nm for β and 0.490nm for TiC. The grain growth seems to be suppressed in 0.5C by the pinning of intergranular TiC particles. The grain boundary pinning must be the reason why deformation texture remained after the solution treatment. These microstructural features obtained are summarized in Table 1.

Shape memory properties. Figure 5 show cyclic loading-unloading tensile stress-strain curves of (a) Ti-27Nb, (b) 0.2C and (c) 0.5C, respectively. Superelasticity appeared in Ti-27Nb, but it did not clearly seen in 0.2C and 0.5C. The disappearance of superelasticity is possibly caused by (1) the decrease in M_s due to solute carbon and/or (2) inhibition of martensitic transformation due to TiC obstacles. Probably, since the carbon solubility in Ti-27Nb is very small, the disappearance is though to be due to TiC particles. It is also obvious that the flow-stress becomes higher with increase in carbon content. In order to

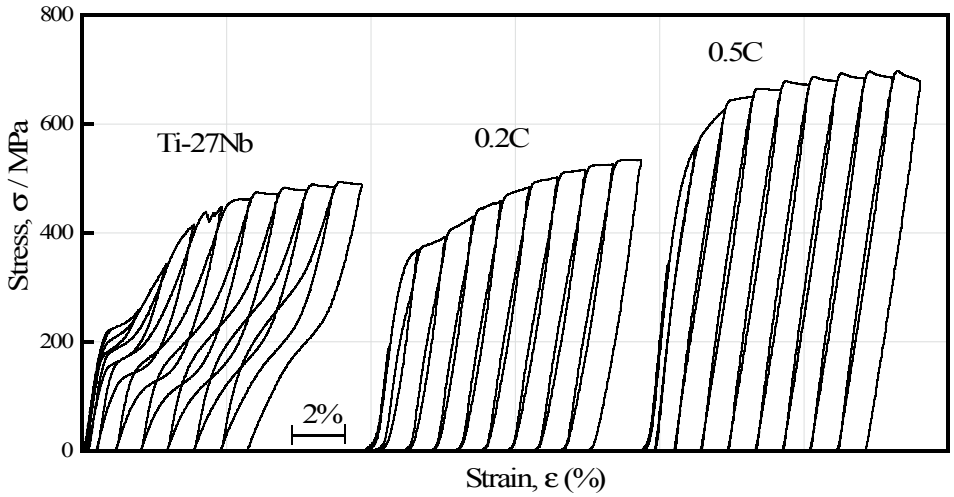

Figure 5 Cyclic loading-unloading tensile stress-strain curves.

clarify the effect of carbon addition on strength, permanent plastic (residual) strain was plotted in Figure 6 against the maximum applied stress in each loading-unloading deformation cycle. These stress-strain curves in Fig. 6 correspond to usual stress-strain curves when deformed by slip. Using Fig.6, 0.2% flow stress was evaluated and plotted as a function of carbon content as shown in Figure 7. The 0.2% flow stress of Ti-27Nb was 340MPa, and it linearly increased with carbon content: 420MPa for 0.2C and 540MPa for 0.5C. The strength increment rate by carbon addition is evaluated to be 400MPa/mass%C. By taking into account that carbides do not affect the yield stress in Ti-Ni [15], the hardening by carbon in this work is probably caused by grain refinement for the most part, and dispersion hardening by TiC particles and solid solution hardening by carbon atoms in β matrix for the rest. Grain refinement is an important factor for the strengthening, and the strength usually obeys the Hall-Petch equation, that is,

$$\sigma_{0.2} = \sigma_0 + k\, d^{-1/2} \quad (1),$$

where $\sigma_{0.2}$ is the yield stress, σ_0 and k are material constants, and d is the grain size. Figure 8 shows Hall-Petch plot. Although the linearity in Fig.7 is not good and the number of data is a few, σ_0 and k are evaluated to be 165 MPa and 1322 MPa $\mu m^{1/2}$, respectively. Besides, TiC particles may enhance the strength due to dispersion hardening. Solid solution strengthening by carbon seems not so important, because the carbon content in β matrix should be considerably small due to the limited solid solubility. Another reason is that same degree in solid solution hardening should be expected in both 0.2C and 0.5C, although different strength was recognized in these alloys. Regardless of hardening mechanism, carbon addition raises the critical stress for slip of Ti-Nb alloys, and it is effective to reduce the grain size. However, carbon addition suppresses the martensitic transformation due to TiC particles. A proper amount of carbon content may be more effective to enhance mechanical properties without degradation of superelasticity.

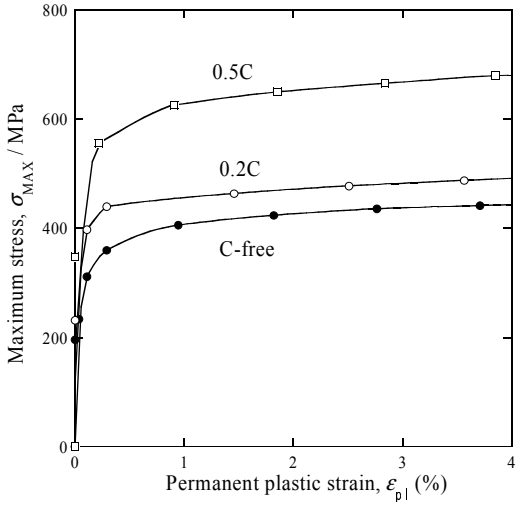

Figure 6 Relationships between permanent plastic strain and maximum stress using Fig.5.

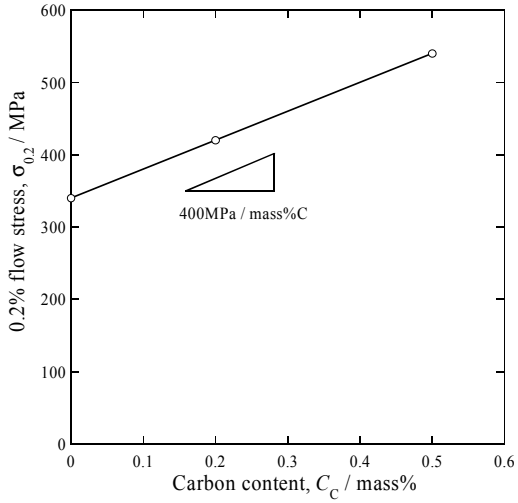

Figure 7 0.2% flow stress as a function of carbon content.

Conclusions

(1) β (bcc) parent phase was formed in Ti-27mol%Nb alloys at room temperature, and NaCl type TiC existed in C-added alloys.
(2) The grain size of Ti-27Nb, 0.2C and 0.5C after the solution treatment at 1273K for 1.8ks were 63μm, 23μm and 15μm, respectively. The grain size was decreased with carbon

content. The grain size reduction must be due to grain boundary pinning by TiC.
(3) Strong $\{112\}_\beta<110>_\beta$ recrystallization texture was formed in solution-treated Ti-27Nb. On the other hand, weak $\{001\}_\beta<110>_\beta$ texture was formed in 0.5C. This is due to the recrystallization is suppressed by TiC particles.
(4) Stress-induced martensitic transformation seemed to be suppressed by TiC particles in C-added alloys.
(5) The critical stress for slip was linearly increased by carbon content. The increase was 400MPa/mass%C.
(6) Carbon addition is effective to increase the critical stress for slip and to suppress the grain growth of Ti-Nb alloys.

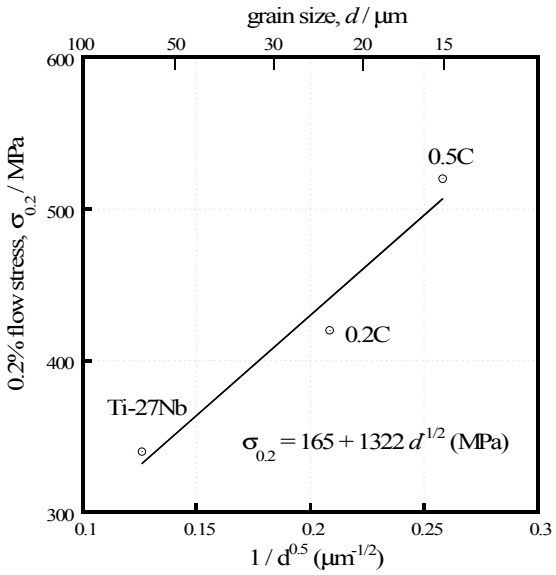

Figure 8 Hall-Petch plot for Ti-27Nb base alloys.

Acknowledgment

This work was supported by a Grant-in-Aid for Fundamental Scientific Research Kiban B (No.20360310, 2008-2010) from the Ministry of Education, Culture, Sports, Science and Technology, Japan.

References

[1] S. Miyazaki, H. Y. Kim and H. Hosoda: Mat. Sci. Eng. A **438-440** (2006) p.18.
[2] A. R. G. Brown, D. Clark, J. Eastabrook and K. S. Jepson: Nature **201** (1964) p.914.
[3] T. Inamura, J. I. Kim, H. Y. Kim, H. Hosoda, K. Wakashima and S. Miyazaki: Philos. Mag., **87** (2007) p.3325.
[4] C. Baker: Metal Sci. *J.*, **5** (1971) p.92.
[5] H. Y. Kim, H. Satoru, J. I. Kim, H. Hosoda and S. Miyazaki: Mat. Trans. **45** (2004) p.2443.
[6] Y. Fukui, T. Inamura, H. Hosoda, K. Wakashima and S. Miyazaki: Mat. Trans. **45** (2006) p.1077.
[7] J. I. Kim, H. Y. Kim, T. Inamura, H. Hosoda and S. Miyazaki: *Mat. Trans.* **47** (2006) p.505.
[8] S. Miyazaki: Materia Japan **35** (1996) p.179.
[9] J. I. Kim, H. Y. Kim, H. Hosoda and S. Miyazaki: Mat. Trans. **46** (2006) p.852.
[10] Y. Horiuchi, T. Inamura, H. Hosoda, K. Wakashima, H. Y. Kim and S. Miyazaki: Mat. Sci. Eng. A **438-440** (2006) p.830.
[11] H. Y. Kim, Y. Ikehara, J. I. Kim, H. Hosoda and S. Miyazaki: Acta Mater. **54** (2006) p.2419.
[12] in: *Binary Alloy Phase Diagrams*, ed. By T. B. Massalski, Vol.1, p.577 (C-Nb) and p.593 (C-Ti), ASM, USA (1986).
[13] T. Inamura, Y. Fukui, H. Hosoda, K. Wakashima and S. Miyazaki: Mat. Sci. Eng. C **25** (2005) p.426.
[14] D. L. Moffat and D. C. Larbalestier: Metall. Trans. A **19A** (1988) p.1677.
[15] T. Saburi: in *Shape Memory Materials*, ed. by K. Otsuka and C. M. Wayman, Chapter 3, p.49, Cambridge University Press, UK (1998).

THERMEC 2009
doi:10.4028/www.scientific.net/MSF.638-642

Effect of Carbon Addition of Shape Memory Properties of TiNb Alloys

doi:10.4028/www.scientific.net/MSF.638-642.2046

References

[1] S. Miyazaki, H. Y. Kim and H. Hosoda: Mat. Sci. Eng. A 438-440 (2006) p.18.
doi:10.1016/j.msea.2006.02.054

[2] A. R. G. Brown, D. Clark, J. Eastabrook and K. S. Jepson: Nature 201 (1964) p.914.
doi:10.1038/201914a0

[3] T. Inamura, J. I. Kim, H. Y. Kim, H. Hosoda, K. Wakashima and S. Miyazaki: Philos. Mag., 87 (2007) p.3325.
doi:10.1080/14786430601003874

[4] C. Baker: Metal Sci. J., 5 (1971) p.92.

[5] H. Y. Kim, H. Satoru, J. I. Kim, H. Hosoda and S. Miyazaki: Mat. Trans. 45 (2004) p.2443.
doi:10.2320/matertrans.45.2443

[6] Y. Fukui, T. Inamura, H. Hosoda, K. Wakashima and S. Miyazaki: Mat. Trans. 45 (2006) p.1077.
doi:10.2320/matertrans.45.1077

[7] J. I. Kim, H. Y. Kim, T. Inamura, H. Hosoda and S. Miyazaki: Mat. Trans. 47 (2006) p.505.
doi:10.2320/matertrans.47.505

[8] S. Miyazaki: Materia Japan 35 (1996) p.179.

[9] J. I. Kim, H. Y. Kim, H. Hosoda and S. Miyazaki: Mat. Trans. 46 (2006) p.852.
doi:10.2320/matertrans.46.852

[10] Y. Horiuchi, T. Inamura, H. Hosoda, K. Wakashima, H. Y. Kim and S. Miyazaki: Mat. Sci. Eng. A 438-440 (2006) p.830.
doi:10.1016/j.msea.2006.02.058

[11] H. Y. Kim, Y. Ikehara, J. I. Kim, H. Hosoda and S. Miyazaki: Acta Mater. 54 (2006) p.2419.
doi:10.1016/j.actamat.2006.01.019

[12] in: Binary Alloy Phase Diagrams, ed. By T. B. Massalski, Vol.1, p.577 (C-Nb) and p.593 (C-Ti), ASM, USA (1986).

[13] T. Inamura, Y. Fukui, H. Hosoda, K. Wakashima and S. Miyazaki: Mat. Sci. Eng. C 25 (2005) p.426.
doi:10.1016/j.msec.2005.01.025

[14] D. L. Moffat and D. C. Larbalestier: Metall. Trans. A 19A (1988) p.1677.

[15] T. Saburi: in Shape Memory Materials, ed. by K. Otsuka and C. M. Wayman, Chapter 3, p.49, Cambridge University Press, UK (1998).